THE JOURNAL OF PHYSICAL CHEMISTRY C

Article

pubs.acs.org/JPCC

Electron-Transfer Kinetics through Interfaces between Electron-Transport and Ion-Transport Layers in Solid-State Dye-Sensitized Solar Cells Utilizing Solid Polymer Electrolyte

Woohyung Cho,[†] Jongchul Lim,[‡,#] Tea-Yon Kim,[†] Young Rae Kim,[†] Donghoon Song,[†] Taiho Park,[*,‡] Francisco Fabregat-Santiago,[*,∥] Juan Bisquert,[∥,⊥] and Yong Soo Kang[*,†]

[†]Center for Next Generation Dye-Sensitized Solar Cells, Department of Energy Engineering, Hanyang University, 133-791, Seoul, Republic of Korea

[‡]Department of Chemical Engineering, Pohang University of Science and Engineering, 790-784, Pohang, Republic of Korea

[∥]Institute of Advanced Materials (INAM), Universitat Jaume I, 12071 Castelló, Spain

[⊥]Department of Chemistry, Faculty of Science, King Abdulaziz University, Jeddah, Saudi Arabia

Supporting Information

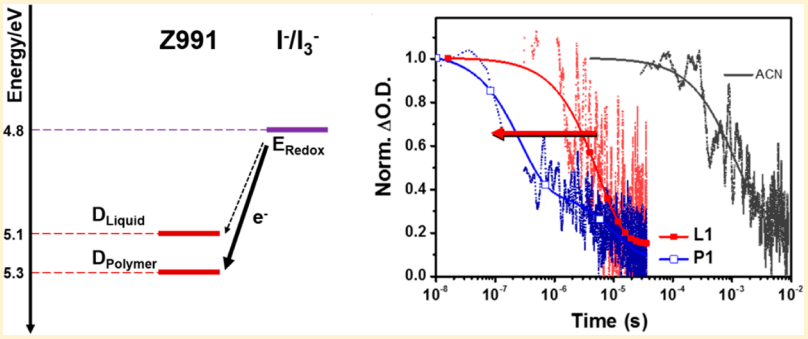

ABSTRACT: The origin of the differences between the performance parameters found for dye-sensitized solar cells (DSCs) using liquid and poly(ethylene oxide)-based solid polymer electrolytes has been investigated. Limitations associated with poor polymer electrolyte penetration and ionic diffusion have been analyzed together with other effects such as the dye regeneration rate, the conduction band edge shift, and the electron recombination kinetics occurring in the solid polymer electrolyte. We have found that dye regeneration was faster for sensitized TiO_2 films fully wetted with polymer electrolyte than that with liquid cells. This new result was attributed to a 0.2 eV decrease in the dye highest occupied molecular orbital energy yielding to an increase in the driving force for dye regeneration. These understandings may contribute to a further increase in the energy-conversion efficiency of DSCs employing solid polymer electrolyte.

INTRODUCTION

Dye-sensitized solar cells (DSCs) have received much attention due to their attractive features such as high energy-conversion efficiency and low production costs. Their energy-conversion efficiency was recorded up to 14.0%[1] under 1 sun conditions with YD-o-C8 dye and cobalt complex redox couples dissolved in liquid volatile solvent; however, the practicability of DSCs with liquid electrolyte remains a challenge. Thus, considerable efforts have been made to realize devices with high efficiencies that meet the stability criteria for outdoor use by replacing the liquid electrolyte with solid-state polymer electrolyte (P). In addition, problems associated with dye detachment may not be serious compared to liquid electrolytes, and relatively high energy-conversion efficiency can be observed under low light intensity.[2] Furthermore, for device commercialization, polymer redox electrolytes provide the required mechanical strength and flexibility to endure bending stress, which is quite advantageous for both the roll-to-roll process and flexible devices.[3] However, the power-conversion efficiencies of DSCs based on solid polymer electrolyte are still much lower than those of the corresponding cells with liquid electrolytes due to the diffusion limitation[4,5] and poor interfacial contact with dyes. Therefore, there have been several different approaches to improve the ionic conductivity through solid polymer electrolytes. For example, the ionic conductivity can be readily improved by incorporating nanosized inorganic materials mainly due to the generation of free volume at the interface between the solid polymer electrolyte and nanoparticles.[6] The addition of nanoparticles may also inhibit the crystallization of the polymer and consequently enhance its ionic conductivity.[7,8] The poor interfacial contact of solid polymer electrolyte with dyes mostly come from the difficulty in penetration of the large-sized

Received: September 23, 2015
Revised: January 8, 2016

DOI: 10.1021/acs.jpcc.5b09259
J. Phys. Chem. C XXXX, XXX, XXX−XXX

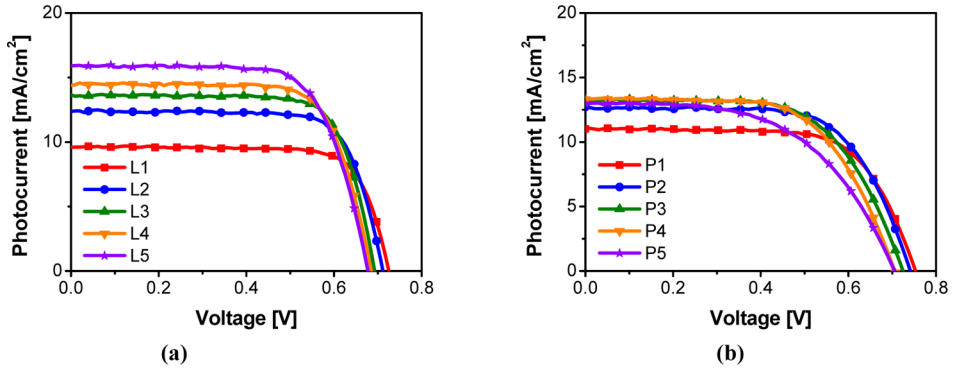

Figure 1. Photovoltaic performances of DSCs with (a) liquid electrolyte and (b) PEO-based solid polymer electrolyte by varying the number of TiO_2 layers (each layer thickness ~4 μm) under 1 sun illumination (100 mW cm^2 and AM 1.5 G) with shadow mask and 0.25 cm^2.

polymer electrolyte chains (~100 nm) into nanopores (~20 nm) of TiO_2 layer. Poor pore penetration or filling of polymer electrolyte has been improved by utilizing small-sized oligomers (<5 nm) and subsequent self-solidification by multiple hydrogen bonds, nanoparticles, or polymers; this strategy is called the "oligomer approach".[9]

The employment of solid polymer electrolyte such as poly(ethylene oxide) (PEO)-based electrolyte can significantly enhance open-circuit voltage (V_{OC}) for DSCs.[5,10,11] According to previous research, the negative shift of the conduction band edge of TiO_2 and the suppression of charge recombination at the TiO_2/electrolyte interface in DSCs with polymer electrolyte have been considered to be the major factors leading to the improvement of V_{OC}.[12] Therefore, the low efficiency in DSCs employing solid polymer electrolyte mostly comes from both low short-circuit current density J_{SC} and fill factor (FF).

In this work, we quantitatively studied the effects of the pore penetration of PEO-based solid polymer electrolyte and its ionic conductivity on the photovoltaic performance of DSCs, especially emphasized on J_{SC}, because its limitation appears to be a major reason not to have high efficiency. Since the dye-regeneration kinetics is strongly affected by the accessibility of I^- ions to the dye and the electron injection depends strongly on the alignment of the dye lowest unoccupied molecular orbital energy with respect to the conduction band energy level (E_c) of TiO_2 layer, we investigate the origin of J_{SC}, by characterization through dye-regeneration rate with nanosecond−millisecond transient absorption spectroscopy, electrochemical impedance spectroscopy, and intensity-modulated photovoltage spectroscopy. The dye-regeneration rate with the solid polymer electrolyte is, surprisingly, nearly 10 times faster than that for a common liquid one, when the mesopores of the TiO_2 layer are completely filled (<4 μm), while the electron recombination rate is slower for the former than for the latter. Such results are explained by the 0.2 eV downward highest occupied molecular orbital (HOMO) level shift of the dye, accompanied by the 0.3 V downward shift in the conduction band of TiO_2.

EXPERIMENTAL DETAILS

Device Fabrication. Fluorine-doped tin oxide (FTO) glass plates (Pilkington-TEC8, St. Helens, England) were cleaned using an ultrasonic bath on the order of 2 vol % of Helmanex, deionized water, and ethanol. Screen-printed layer of 20 nm TiO_2 particles (PST-18 NR, CCIC, Osaka, Japan) were used as photoelectrodew. A 4 μm thick film per 1 layer for transparent film was coated on the conducting glass electrode. The TiO_2 electrodes were repeated 1−5 times and heated at 450 °C for 30 min. TiO_2-coated electrodes were treated with a 0.5 mM $TiCl_4$ solution for 20 min at 70 °C, followed by an annealing process for 30 min at 450 °C. Following heat treatment, these electrodes were immersed into the 0.3 M Z991 (cis-di(thiocyanato)bis(2,2′-bipyridyl-4,4′-dicarboxylate) (4,4′-bis-(5-(5-octyl-thiophen-2-yl)thiophen-2-yl)-2,2′-bipyridine) ruthenium(II)) dye solution with 0.3 mM dineohexyl bis(3,3-dimethylbutyl)phosphinic acid (DINHOP) in acetonitrile (ACN, Wako, Richmond, VA)/*tert*-butylalcohol (tBuOH, Wako) (1/1, volume ratio) and kept at room temperature. The TiO_2 electrode was rinsed with ACN and dried. The Pt electrode was prepared by spin coating of 10 mM H_2PtCl_6 (Sigma-Aldrich) in 2-propanol (Sigma-Aldrich) and then sintered at 450 °C for 30 min. The dye-coated TiO_2 electrode and counter electrode were assembled with Surlyn (25 μm, DuPont, Wilmington, DE). The dye-sensitized TiO_2 active area was 0.25 cm^2.

Electrolyte Preparation. The liquid electrolyte was composed of 0.6 M 1-methyl-3-propylimidazolium iodide (MPII, Sigma-Aldrich) and 0.05 M iodine (Sigma-Aldrich) in ACN. The polymer electrolyte was based on a 6/4 mix of poly(ethylene glycol)dimethyl ether (PEGDME, molecular weight (M.W.) 500, Sigma-Aldrich)/poly(ethylene oxide) (PEO, M.W. 600 000, Sigma-Aldrich) with 0.6 M MPII and 0.05 M I_2.

Characterization. To determine the properties of photovoltaic performance, the current−voltage (J−V) characteristics of DSCs were measured with a Keithley Model 2400 source meter (Cleveland, OH) and a solar simulator, with a 300 W xenon arc lamp (Newport Corporation, Irvine, CA) under 1 sun illumination (AM 1.5, 100 mW/cm^2). A light-shading mask, placed on the residual area of the front side of the FTO substrate (except for the 0.25 cm^2 TiO_2 active area), was employed to prevent overestimation of the power-conversion efficiency. The diffusion coefficients were determined by measurement of limiting current in a linear sweep voltammetry (LSV) using an Autolab instrument (320N) with 1 mV/s scan rates.[13] Differential pulse voltammograms of the Z991 sensitizer with solvent were measured in a solution containing 0.1 M lithium perchlorate using a three-electrode apparatus comprising a platinum plate counter electrode, a platinum working electrode, and a Ag/AgCl (saturated aqueous KCl) reference electrode. Z991 sensitizer was dissolved in ACN, 1 wt % PEGDME in ACN, and 1 wt % of PEGDME/PEO (6/4, w/w) at a concentration of 0.03 mM.[14] The electron lifetime, density of states, and chemical capacitance were characterized by

DOI: 10.1021/acs.jpcc.5b09259
J. Phys. Chem. C XXXX, XXX, XXX−XXX

Table 1. Diffusion Coefficient of I_3^- and Photovoltaic Performances for Liquid and Solid Polymer Electrolytes

electrolyte	diffusion coefficient of I_3^- ($cm^2\ s^{-1}$)	sample	number of TiO_2 layers[a]	V_{OC} (V)	J_{SC} (mA cm^{-2})	FF	η (%)
liquid (L)	8.35×10^{-5}	**L1**	1	0.72	9.6	0.77	5.3
		L2	2	0.71	12.4	0.75	6.6
		L3	3	0.69	13.6	0.76	7.1
		L4	4	0.68	14.4	0.74	7.3
		L5	5	0.68	15.9	0.70	7.6
solid polymer electrolyte (P)	2.23×10^{-7}	**P1**	1	0.75	11.0	0.69	5.7
		P2	2	0.74	12.7	0.66	6.3
		P3	3	0.72	13.3	0.63	6.0
		P4	4	0.71	13.3	0.63	5.9
		P5	5	0.71	13.0	0.55	5.0

[a]Each layer is approximately 4 μm thick.

electrochemical impedance spectroscopy using the Autolab instrument (320N, Utrecht, The Netherlands) measuring at bias potential between 0 and 0.9 V.[15,16] Pulsed laser excitation was applied using a Continuum Surelite-II Q-switched Nd:YAG laser (λ = 355 nm, 10 Hz repetition rate, San Jose, CA). The output of the optical parametric oscillator (pulse width at half-height, 6 ns) was tuned at 532 nm and attenuated to 75 $\mu J/cm^2$ pulse. The analyzer light, produced by a 150 W Xe arc lamp, was passed through the sample and was detected by the amplifier-equipped Si photodiode. A 1 GHz band-pass digital signal analyzer was employed to record the time course of the optical absorbance changes induced by the laser excitation of the films. Satisfactory signal-to-noise ratios were typically obtained by averaging over 512 laser shots.[17,18]

RESULTS AND DISCUSSION

Photovoltaic Performance. The photovoltaic performance of DSCs by varying the TiO_2 thickness (each TiO_2 layer is ~4 μm thick) for both liquid and solid polymer electrolytes was evaluated (Figure 1). The photovoltaic parameters, including the open-circuit voltage (V_{OC}), short-circuit current density (J_{SC}), fill factor (FF), and overall energy-conversion efficiency (η), are listed in Table 1. The maximum efficiency is 6.3% for DSC with solid polymer electrolyte (P-DSC) and two layers of the TiO_2 film, whereas DSC with the liquid electrolyte (L-DSC) exhibited the highest efficiency of 7.6% with five layers of the TiO_2 film. The lower efficiency with P-DSC is mostly attributable to lower J_{SC} and FF despite the increase in V_{OC}, compared to that of the L-DSC.

In the case of the liquid electrolyte, J_{SC} increases quite linearly with the number of TiO_2 layers as expected, meaning that most of the dyes adsorbed on the TiO_2 are active and contribute to the cell performance. However, for P-DSC, J_{SC} increases with the number of TiO_2 layers until reaching a plateau when the number of TiO_2 layers is larger than 2. This result may be associated with the fact that only part of the dyes adsorbed are able to contribute to the cell performance with a large number of TiO_2 layers, suggesting incomplete penetration of the solid polymer electrolyte into the mesopores of TiO_2. Another consequence of poor contact between the solid electrolyte and the dyes may also be a limitation in the regeneration of the oxidized dye molecules.[11]

In the case of only one TiO_2 layer, the efficiency of DSC with the solid polymer electrolyte (**P1**) is higher than that with the liquid electrolyte (**L1**). This may be attributable to the electrolyte composition that while it is optimized for the polymer, it is not for the liquid cell. However, for the comparison for liquid and solid polymer electrolytes, it was necessary that both electrolytes had the same salt contents.

To determine the origin of the behavior of the cells described above, several transient techniques such as LSV, impedance spectroscopy (IS), or transient absorption spectroscopy (TAS) were used

From the measurement of the limiting current density in LSV using a blank cell, 10.8 mA·cm^{-2} in Pt-FTO//electrolyte (60 μm thick)//Pt-FTO, it was found that the diffusion coefficient of the I_3^- ions through the liquid electrolyte is almost 2 orders of magnitude faster than that through the solid polymer electrolyte as listed in Table 1. As the I_3^- ion diffuses slowly in P-DSC, the regeneration of the oxidized dye might also be limited, resulting also in a lower J_{SC} value than that for L-DSC. However, the values obtained for J_{SC} in complete cells are far from the diffusion limit as the polymer thickness is in this case 20 μm. To understand the effects of the slow diffusion coefficient through the polymer electrolyte on J_{SC}, we carried out time-response photocurrent transient measurements for both L-DSC and P-DSCs by varying the TiO_2 film thickness as shown in Figure S2.[19] For L-DSCs, the photocurrent remained unchanged regardless of the film thickness, whereas P-DSC showed a sharp decrease in the photocurrent with time and the slope became stiffer with the increase in the number of TiO_2 layers. Such different behavior between L- and P-DSCs is mostly attributable to the difference in the ion diffusion kinetics. A secondary effect of slow ion motion in polymer cell is the increase in the diffusion resistance, resulting in a decrease in FF of P-DSC observed in Table 1. As expected, this decrease in FF is larger for both higher current and thicker films.[20−22]

IS has been proven to be a powerful technique for investigating conduction band shifts and electron recombination through the analysis of chemical capacitance (C_μ) and recombination resistance (R_{rec}).[20−23] Here, these parameters will be investigated and further analysis will be extended to examine the density of states (DOS) given by

$$\mathrm{DOS} = \frac{q^2}{kT}\frac{C_\mu}{d(1-p)} \tag{1}$$

and the electron lifetime, which is

$$\tau_e = R_{rec}C_\mu \tag{2}$$

q, d, and p are respectively electron charge, thickness of TiO_2 layer, and porosity.

Figure 2a shows chemical capacitance C_μ for the different configurations of DSCs. It is observed that the thicker the TiO_2 layer, the larger the chemical capacitance, except for the case of

DOI: 10.1021/acs.jpcc.5b09259
J. Phys. Chem. C XXXX, XXX, XXX−XXX

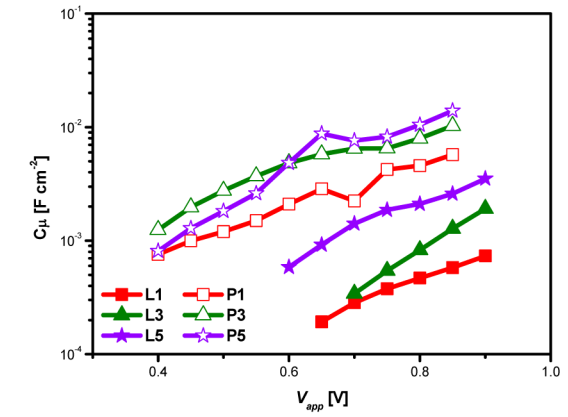

(a)

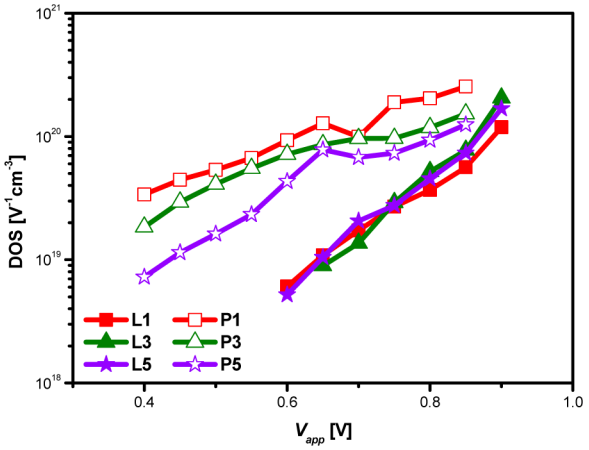

(b)

Figure 2. (a) Chemical capacitance and (b) density of trap states of DSCs by varying the TiO_2 film thickness using liquid (**L1**, **L3**, and **L5**) and solid polymer electrolytes (**P1**, **P3**, and **P5**) from the data obtained from IS.

P5. In all cases, C_μ presents larger values for polymer electrolytes than for the liquid ones, suggesting that the conduction band is downwardly shifted to a lower value in the case of solid polymer electrolyte. When the value of C_μ is normalized to the volume of TiO_2 film to obtain DOS from eq 1, as plotted in Figure 2b, thickness effects are revealed more precisely. As expected, DOS of all liquid electrolyte samples is the same regardless of the thickness of the TiO_2 layer, indicating that all dyes adsorbed on the TiO_2 film surface are active (i.e., good contact between dyes and electrolyte). However, the polymer electrolyte shows a decrease in DOS with increasing TiO_2 film thickness, indicating that only part of the adsorbed dyes are active (disconnected from electrolyte) already for three layers (~12 μm).

Both J_{SC} and DOS data suggest that **P1** has good penetration by the polymer electrolyte. Therefore, if we assume full TiO_2 polymer wetting, it is possible to estimate that the shift in the conduction band of TiO_2 upon contacting with the polymer electrolyte with respect to the liquid one is $\Delta E_c \sim +0.3$ eV, with the plus sign indicating downward direction.

Despite this large decrease in conduction band, V_{OC} becomes however larger for polymer electrolytes than for liquid ones. The origin of this phenomenon may be explained with the help of recombination resistance as shown in Figure 3. At low applied potentials, when recombination is dominated by charge

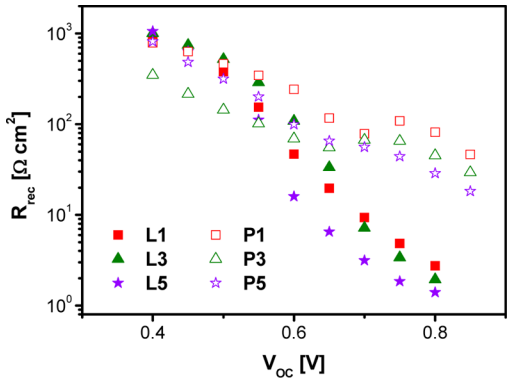

Figure 3. Recombination resistance vs applied voltage by varying the TiO_2 film thickness using liquid (**L1**, **L3**, and **L5**) and solid polymer electrolytes (**P1**, **P3**, and **P5**) measured by the IS method.

transfer at the boundary FTO/TiO_2/dye/electrolyte interface, R_{rec} is nearly the same for all samples. However, around V_{OC} (0.65−0.75 V), where recombination is dominated by charge transfer at the bulk of TiO_2 nanoparticles/electrolyte, R_{rec} is larger for polymer electrolyte than for liquid electrolyte DSCs that yields to the higher value of V_{OC} despite the differences in J_{SC}.[24] This result indicates that the kinetics of recombination to I_3^- in P-DSC is much slower than that in for L-DSC, which agrees well with the lifetime results in Figure S2, where the applied voltage has been shifted 300 mV for the case of the liquid electrolyte, to adjust the conduction band shift. As observed, the polymer electrolyte presents a much longer lifetime than the liquid electrolyte DSCs.

The origin of this slower recombination kinetics may be attributed to the passivation of TiO_2 interface by the polymer chains.[3] Another possible explanation could be the slower ion transport (see Figure S3) and, consequently, the lower recombination probability of TiO_2 electrons with I_3^- ion in polymer electrolyte.

Pore Penetration. The penetration of electrolyte through mesopores of the TiO_2 layer is verified by TAS. The oxidized dye D^+ can be reduced by electrons coming from the oxidation reaction of I^- and/or the photoelectrons in the TiO_2 layer. The former is referred to as the dye-regeneration reaction and the latter the electron recombination to dye. In the absence of the redox couples such as I_3^-/I^-, the only reduction path for D^+'s is electron recombination. One common way to characterize the dye-regeneration rate is therefore to compare the decay rate of D^+ band with and without the redox couple by TAS.[25] The decay of the variation in optical density associated with D^+ is solely related to the recombination reaction in the absence of redox couple, generally occurring on the micro- to millisecond time scale. On the other hand, in the presence of redox couple, the decay in the optical density for D^+ is associated with both the dye regeneration and the recombination reaction mentioned above.[26]

Normalized optical density decay (ΔO.D.) of oxidized dye D^+ in both L- and P-DSCs by varying the number of TiO_2 layers (**L1**, **L3**, **L5**, **P1**, **P3**, and **P5**) was probed at the wavelength of 820 nm using transient absorption spectroscopy, representing the metal-to-ligand charge transfer (MLCT) associated with the ligand-localized D^+, upon excitation at 532 nm (the maximum absorption of the Z991 dye) (Figure S4). Figure 3a shows ΔO.D. of D^+ for **L1** and **P1** as a function of time, compared with the control device without redox couple

DOI: 10.1021/acs.jpcc.5b09259
J. Phys. Chem. C XXXX, XXX, XXX−XXX

in acetonitrile. The estimated half time (at 0.5 ΔO.D.) for D^+ without redox couple was ~1.2 ms, nearly 2−3 orders of the magnitude longer than for both L- and P-DSCs with the I^-/I_3^- redox couples as shown in Figures 2a and S4. This indicates that the reduction of D^+'s is dominated by the dye-regeneration process through the oxidation reaction of I^-, regardless of liquid or solid polymer electrolyte. This result is consistent with the previous report in which the rate of the dye regeneration (ca. $\sim 10^6$ /s) was much faster than the recombination reaction rate to dye (ca. $\sim 10^3$/s).[27,28,12]

The thickness of the photoelectrode also influences the regeneration of D^+.[18,29−31] The dye-regeneration rate of P-DSCs becomes slower with increasing the thickness of the electron-transport layer, unlike L-DSCs showing the similar dye-regeneration rate as shown in Figure S4. These results for P-DSCs suggest that the pores may not be completely wetted with the solid polymer electrolyte from the top to the bottom, especially the deeper pores, consequently slowing the dye-regeneration process.[32] Low ionic conductivity of I^- in polymer electrolyte would have similar effects;[3] however, chemical capacitance behavior described above discards this alternative explanation of the main limitation of D^+ regeneration.

An important result arises from the comparison of the estimated half lifetime of 0.50 ± 0.03 μs for **P1**, which was 1 order of magnitude shorter than that for **L1** as shown in Figure 2a. In previous studies, it has been frequently suggested that DSCs based on solid polymer electrolyte show slower dye-regeneration rate than those based on liquid electrolyte due to its slow ionic conductivity. But this is not the case for the current P-DSC device **P1**, whose mesopores were filled completely with polymer electrolyte.[30,33] As can be observed in Figure S4b, this is not the case for the samples with incomplete polymer filling (**P3** and **P5**). As expected, the increased amount of the dye not accessed by the solid polymer electrolyte decreases the dye-regeneration rate, which is consistent with results given above.

HOMO Level Shift. For further analysis on the dye-regeneration rate, the HOMO level shift of the dye was studied using differential pulse voltammetry. Figure 4b illustrates the differential pulse voltammograms obtained with Z991 dye in a varying solvent of ACN, PEGMDE, and PEO/PEGDME under the scanning range of 0 to +1.5 V (vs Ag/AgCl).[14] The voltammograms, showing the HOMO level of a dye depending on solvent, indicates a positive shift of +0.2 V from the liquid electrolyte of ACN to the solid polymer electrolyte of PEGDME or (PEO + PEGDME). The positive or downward shift of the HOMO level of the dye in the solid polymer electrolyte indicates an increase in the energetic driving force for the regeneration of the oxidized dye. For fast dye regeneration by iodide ion, the large driving force would be necessary to overcome the mechanistic complexity of the two-electron redox process involved with the iodide redox copule.[34] Therefore, it is suggested that the regeneration rate for **P1** is faster than that of **L1** as shown in Figure 4a due to the increased driving force for the dye regeneration, despite the faster ionic conductivity in the liquid electrolyte than in the solid polymer electrolyte. The faster dye-regeneration rate in **P1** may consequently lead to the higher J_{SC} of **P1** than that of **L1**.

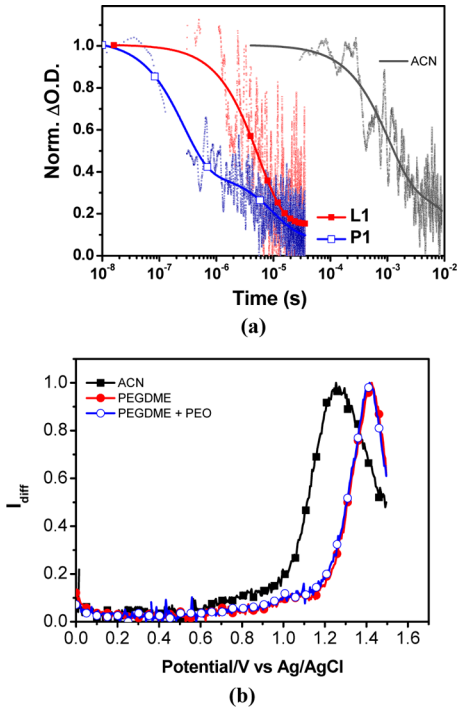

Figure 4. Normalized optical density decay (ΔO.D.) profiles of D^+ for DSCs: (a) One layer of TiO_2 with liquid and solid polymer electrolytes (**L1** and **P1**) in comparison with the control device (ACN), probed at 820 nm using transient absorption spectroscopy. (b) Normalized differential pulse voltammograms of Z991 with different solvent.

CONCLUSIONS

In this paper, the origin of the differences in photovoltaic performance parameters between liquid and solid polymer electrolytes by varying the various thicknesses of the TiO_2 electron-transport layer has been investigated in terms of the ionic conductivity, the pore penetration of the electrolyte, conduction band edge shifts, and recombination kinetics. The TAS data suggested that the PEO-based polymer electrolyte could fill the mesopores of the common TiO_2 layer reasonably well when its thickness is lower than 4 μm. In addition, the reduction rate of D^+ was found to be dominated by the dye regeneration, rather than the electron recombination. Furthermore, the dye-regeneration rate with the solid polymer electrolyte was surprisingly nearly 10 times faster than that for the liquid one, when the mesopores of the TiO_2 layer was filled completely (<4 μm), while the electron recombination rate was slower for the former than for the latter. The faster regeneration rate for the solid polymer electrolyte appears to be associated with its increased driving force due to the 0.2 eV downward HOMO level shift of the dye as evidenced by differential pulse voltammograms and despite its 2 orders of magnitude lower ionic conductivity, measured and confirmed by linear sweep voltammetry and the photocurrent transient behavior, respectively. Interestingly, the downward shift of the dye HOMO is accompanied by the 0.3 V downward shift in the conduction band of TiO_2 that ensures good injection of photogenerated electrons in thin polymeric samples.

ASSOCIATED CONTENT

Supporting Information

The Supporting Information is available free of charge on the ACS Publications website at DOI: 10.1021/acs.jpcc.5b09259.

DOI: 10.1021/acs.jpcc.5b09259
J. Phys. Chem. C XXXX, XXX, XXX−XXX

Additional $J-V$ curves under dark conditions, electron lifetime, photocurrent decay, and TAS data with electrolyte and TiO_2 thickness (PDF)

AUTHOR INFORMATION

Corresponding Authors

*E-mail: kangys@hanyang.ac.kr. Fax: +82 2 2296 2969. Tel.: +82 2 2220 2336 (Y.S.K.).
*E-mail: fran.fabregat@fca.uji.es (F.F.-S.).
*E-mail: taihopark@postech.ac.kr. Tel.: +82 54-279-2394 (T.P.).

Present Address

#Department of Physics, University of Oxford, Clarendon Laboratory, Parks Road, Oxford, OX1 3PU, United Kingdom.

Notes

The authors declare no competing financial interest.

ACKNOWLEDGMENTS

This work was supported by the National Research Foundation of Korea (NRF) grant funded by the Korea Center for Artificial Photosynthesis (KCAP) (No. 2009-0093883).

REFERENCES

(1) Kakiage, K.; Aoyama, Y.; Yano, T.; Oya, K.; Fujisawa, J.-i.; Hanaya, M. Highly-Efficient Dye-Sensitized Solar Cells with Collaborative Sensitization by Silyl-Anchor and Carboxy-Anchor Dyes. *Chem. Commun.* **2015**, *51*, 15894−15897.

(2) Fakharuddin, A.; Jose, R.; Brown, T. M.; Fabregat-Santiago, F.; Bisquert, J. A Perspective on the Production of Dye-Sensitized Solar Modules. *Energy Environ. Sci.* **2014**, *7*, 3952−3981.

(3) Song, D.; Cho, W.; Lee, J. H.; Kang, Y. S. Toward Higher Energy Conversion Efficiency for Solid Polymer Electrolyte Dye-Sensitized Solar Cells: Ionic Conductivity and TiO_2 Pore-Filling. *J. Phys. Chem. Lett.* **2014**, *5*, 1249−1258.

(4) Chen, C.-L.; Teng, H.; Lee, Y.-L. Preparation of Highly Efficient Gel-State Dye-Sensitized Solar Cells Using Polymer Gel Electrolytes Based on Poly(Acrylonitrile-Co-Vinyl Acetate). *J. Mater. Chem.* **2011**, *21*, 628−632.

(5) Cho, W.; Kim, Y. R.; Song, D.; Choi, H. W.; Kang, Y. S. High-Efficiency Solid-State Polymer Electrolyte Dye-Sensitized Solar Cells with a Bi-Functional Porous Layer. *J. Mater. Chem. A* **2014**, *2*, 17746−17750.

(6) Zhou, Y.; Xiang, W.; Chen, S.; Fang, S.; Zhou, X.; Zhang, J.; Lin, Y. Improvements of Photocurrent by Using Modified SiO_2 in the Poly(Ether Urethane)/Poly(Ethylene Oxide) Polymer Electrolyte for All-Solid-State Dye-Sensitized Solar Cells. *Chem. Commun.* **2009**, 3895−3897.

(7) Stergiopoulos, T.; Arabatzis, I. M.; Katsaros, G.; Falaras, P. Binary Polyethylene Oxide/Titania Solid-State Redox Electrolyte for Highly Efficient Nanocrystalline TiO_2 Photoelectrochemical Cells. *Nano Lett.* **2002**, *2*, 1259−1261.

(8) Chae, H.; et al. Chemical Effects of Tin Oxide Nanoparticles in Polymer Electrolytes-Based Dye-Sensitized Solar Cells. *J. Phys. Chem. C* **2014**, *118*, 16510−16517.

(9) Kang, M.-S.; Kim, J. H.; Won, J.; Kang, Y. S. Oligomer Approaches for Solid-State Dye-Sensitized Solar Cells Employing Polymer Electrolytes. *J. Phys. Chem. C* **2007**, *111*, 5222−5228.

(10) Ren, Y.; Zhang, Z.; Fang, S.; Yang, M.; Cai, S. Application of Peo Based Gel Network Polymer Electrolytes in Dye-Sensitized Photoelectrochemical Cells. *Sol. Energy Mater. Sol. Cells* **2002**, *71*, 253−259.

(11) Kang, M.-S.; Kim, J. H.; Kim, Y. J.; Won, J.; Park, N.-G.; Kang, Y. S. Dye-Sensitized Solar Cells Based on Composite Solid Polymer Electrolytes. *Chem. Commun.* **2005**, 889−891.

(12) Wu, C.; Jia, L.; Guo, S.; Han, S.; Chi, B.; Pu, J.; Jian, L. Open-Circuit Voltage Enhancement on the Basis of Polymer Gel Electrolyte for a Highly Stable Dye-Sensitized Solar Cell. *ACS Appl. Mater. Interfaces* **2013**, *5*, 7886−7892.

(13) Chatzivasiloglou, E.; Stergiopoulos, T.; Kontos, A. G.; Alexis, N.; Prodromidis, M.; Falaras, P. The Influence of the Metal Cation and the Filler on the Performance of Dye-Sensitized Solar Cells Using Polymer-Gel Redox Electrolytes. *J. Photochem. Photobiol., A* **2007**, *192*, 49−55.

(14) Funaki, T.; Otsuka, H.; Onozawa-Komatsuzaki, N.; Kasuga, K.; Sayama, K.; Sugihara, H. Systematic Evaluation of Homo Energy Levels for Efficient Dye Regeneration in Dye-Sensitized Solar Cells. *J. Mater. Chem. A* **2014**, *2*, 15945−15951.

(15) Bisquert, J. A Variable Series Resistance Mechanism to Explain the Negative Capacitance Observed in Impedance Spectroscopy Measurements of Nanostructured Solar Cells. *Phys. Chem. Chem. Phys.* **2011**, *13*, 4679−4685.

(16) Fabregat-Santiago, F.; Garcia-Belmonte, G.; Mora-Sero, I.; Bisquert, J. Characterization of Nanostructured Hybrid and Organic Solar Cells by Impedance Spectroscopy. *Phys. Chem. Chem. Phys.* **2011**, *13*, 9083−9118.

(17) Kong, E.-H.; Lim, J.; Chang, Y.-J.; Yoon, Y.-H.; Park, T.; Jang, H. M. Aerosol OT/Water System Coupled with Triiodide/Iodide (I_3^-/I^-) Redox Electrolytes for Highly Efficient Dye-Sensitized Solar Cells. *Adv. Energy Mater.* **2013**, *3*, 1344−1350.

(18) Lim, J.; Kim, T.; Park, T. Fast Cascade Neutralization of an Oxidized Sensitizer by an in Situ-Generated Ionic Layer of I- Species on a Nanocrystalline TiO_2 Electrode. *Energy Environ. Sci.* **2014**, *7*, 4029−4034.

(19) Kuang, D.; Klein, C.; Zhang, Z.; Ito, S.; Moser, J.-E.; Zakeeruddin, S. M.; Grätzel, M. Stable, High-Efficiency Ionic-Liquid-Based Mesoscopic Dye-Sensitized Solar Cells. *Small* **2007**, *3*, 2094−2102.

(20) Schlichthörl, G.; Park, N. G.; Frank, A. J. Evaluation of the Charge-Collection Efficiency of Dye-Sensitized Nanocrystalline TiO_2 Solar Cells. *J. Phys. Chem. B* **1999**, *103*, 782−791.

(21) Martinson, A. B. F.; Góes, M. S.; Fabregat-Santiago, F.; Bisquert, J.; Pellin, M. J.; Hupp, J. T. Electron Transport in Dye-Sensitized Solar Cells Based on Zno Nanotubes: Evidence for Highly Efficient Charge Collection and Exceptionally Rapid Dynamics. *J. Phys. Chem. A* **2009**, *113*, 4015−4021.

(22) Wu, W.-Q.; Liao, J.-Y.; Chen, H.-Y.; Yu, X.-Y.; Su, C.-Y.; Kuang, D.-B. Dye-Sensitized Solar Cells Based on a Double Layered TiO_2 Photoanode Consisting of Hierarchical Nanowire Arrays and Nanoparticles with Greatly Improved Photovoltaic Performance. *J. Mater. Chem.* **2012**, *22*, 18057−18062.

(23) Raga, S. R.; Fabregat-Santiago, F. Temperature Effects in Dye-Sensitized Solar Cells. *Phys. Chem. Chem. Phys.* **2013**, *15*, 2328−2336.

(24) Raga, S. R.; Barea, E. M.; Fabregat-Santiago, F. Analysis of the Origin of Open Circuit Voltage in Dye Solar Cells. *J. Phys. Chem. Lett.* **2012**, *3*, 1629−1634.

(25) Moon, S.-J.; Yum, J.-H.; Humphry-Baker, R.; Karlsson, K. M.; Hagberg, D. P.; Marinado, T.; Hagfeldt, A.; Sun, L.; Grätzel, M.; Nazeeruddin, M. K. Highly Efficient Organic Sensitizers for Solid-State Dye-Sensitized Solar Cells. *J. Phys. Chem. C* **2009**, *113*, 16816−16820.

(26) Kwon, Y. S.; Lim, J.; Song, I.; Song, I. Y.; Shin, W. S.; Moon, S.-J.; Park, T. Chemical Compatibility between a Hole Conductor and Organic Dye Enhances the Photovoltaic Performance of Solid-State Dye-Sensitized Solar Cells. *J. Mater. Chem.* **2012**, *22*, 8641−8648.

(27) Haque, S. A.; Tachibana, Y.; Klug, D. R.; Durrant, J. R. Charge Recombination Kinetics in Dye-Sensitized Nanocrystalline Titanium Dioxide Films under Externally Applied Bias. *J. Phys. Chem. B* **1998**, *102*, 1745−1749.

(28) Katoh, R.; Furube, A.; Barzykin, A. V.; Arakawa, H.; Tachiya, M. Kinetics and Mechanism of Electron Injection and Charge Recombination in Dye-Sensitized Nanocrystalline Semiconductors. *Coord. Chem. Rev.* **2004**, *248*, 1195−1213.

(29) Koster, L. J. A.; Mihailetchi, V. D.; Ramaker, R.; Blom, P. W. M. Light Intensity Dependence of Open-Circuit Voltage of Polymer:-Fullerene Solar Cells. *Appl. Phys. Lett.* **2005**, *86*, 123509.

DOI: 10.1021/acs.jpcc.5b09259
J. Phys. Chem. C XXXX, XXX, XXX−XXX

(30) Park, S.-H.; Lim, J.; Kwon, Y. S.; Song, I. Y.; Choi, J. M.; Song, S.; Park, T. Tunable Nanoporous Network Polymer Nanocomposites Having Size-Selective Ion Transfer for Dye-Sensitized Solar Cells. *Adv. Energy Mater.* **2013**, *3*, 183−183.
(31) Luo, J.; Xu, M.; Li, R.; Huang, K.-W.; Jiang, C.; Qi, Q.; Zeng, W.; Zhang, J.; Chi, C.; Wang, P.; Wu, J. N-Annulated Perylene as an Efficient Electron Donor for Porphyrin-Based Dyes: Enhanced Light-Harvesting Ability and High-Efficiency Co(II/III)-Based Dye-Sensitized Solar Cells. *J. Am. Chem. Soc.* **2014**, *136*, 265−272.
(32) Melas-Kyriazi, J.; Ding, I. K.; Marchioro, A.; Punzi, A.; Hardin, B. E.; Burkhard, G. F.; Tétreault, N.; Grätzel, M.; Moser, J.-E.; McGehee, M. D. The Effect of Hole Transport Material Pore Filling on Photovoltaic Performance in Solid-State Dye-Sensitized Solar Cells. *Adv. Energy Mater.* **2011**, *1*, 407−414.
(33) Freitas, F. S.; Freitas, J. N. d.; Ito, B. I.; Paoli, M.-A. D.; Nogueira, A. F. Electrochemical and Structural Characterization of Polymer Gel Electrolytes Based on a PEO Copolymer and an Imidazolium-Based Ionic Liquid for Dye-Sensitized Solar Cells. *ACS Appl. Mater. Interfaces* **2009**, *1*, 2870−2877.
(34) Daeneke, T.; Mozer, A. J.; Kwon, T.-H.; Duffy, N. W.; Holmes, A. B.; Bach, U.; Spiccia, L. Dye Regeneration and Charge Recombination in Dye-Sensitized Solar Cells with Ferrocene Derivatives as Redox Mediators. *Energy Environ. Sci.* **2012**, *5*, 7090−7099.

DOI: 10.1021/acs.jpcc.5b09259
J. Phys. Chem. C XXXX, XXX, XXX−XXX